2018 IEEE Intelligent Vehicles Symposium (IV)
Changshu, Suzhou, China, June 26-30, 2018

Analysis on Biosignal Characteristics to Evaluate Road Rage of Younger Drivers: A Driving Simulator Study*

Hongyu Hu, Zheng Zhu, Zhenhai Gao, and Rencheng Zheng

Abstract—**This paper focused on biosignal characteristics to analyze road rage of young drivers in a driving simulator experiment. A total of 12 subjects were enrolled during the experimental study. At first, an unfair incident video is utilized to induce the anger emotion of drivers, and then the anger state is recorded based on the Likert anger scale; meanwhile, a physiological recorder is used to acquire electroencephalogram (EEG) and electrocardiogram (ECG) signals of the subjects. In biosignal processing stage, four typical rhythm bands of α, β, δ, and θ are extracted from the original EEG using a digital filter and wavelet packet decomposition, and power spectrums of the four typical rhythm bands are obtained with a fast Fourier transform analysis. In addition, the average heart rate and R-R standard deviation are calculated through a temporal domain analysis from the original ECG signals. Furthermore, the relationships are analyzed between the sex calculated indicators and four angry levels. It indicates that there is a mainly statistical effect of the angry state for typical rhythm bands of α, β, δ, average heart rate and R-R standard deviation, indicating that these features were significantly different for the normal state, light anger, moderate anger, and heavy anger. The research results provide a theoretical basis and data support for driving emotion detection and aggressive driving behavior analyzing.**

I. INTRODUCTION

The road rage always resulted in a substantial role in a risky and aggressive driving, which is therefore recognized to be a contributor to traffic accidents [1]. In China, it indicated that more than 60 percent of the drivers had road rage experiences with an investigation for the 9620 people [2]. In the USA, 90 percent of the drivers had being involved in at least one incident of the aggressive driving [3], because angry drivers are twice as likely to be involved in the accidents [4, 5]. The anger is one of the most common negative emotions during driving. When the irritation occurs, people tends to impulse adventure, against other drivers to generate road rage [6]. The road rage may have an intensive impact on perception, planning, decision and maneuver of the drivers [7]. In fact, an objectively ergonomic assessment of road rage is critically important for the analysis of driving behaviors [8-10].

In the past few years, regarding road rage, a large number of studies had put forward to conduct quantitative analysis of anger emotion, with self-reports, questionnaires and facial expression in both laboratory and on-road studies [11-14]. Recently, physiology-based anger study has gradually become a hot topic, because physiological signals are spontaneous and not subject to manual intervention and can reflect human emotion state objectively [15].

Zhao et al. [16] proposed an emotion recognition method by extracting the individual heartbeats from the wireless signals reflected off the human body. The resulting heartbeats are then used to estimate emotion-dependent features, which feed a machine-learning emotion classifier. The recognition result can reach at an accuracy comparable to the on-body electroencephalogram (EEG) monitors. Healey et al. [17] evaluated stress state of the drivers by measurement of the physiological signals of electrocardiogram (ECG), skin conductivity and respiration during the real-world driving tasks. The results show that for the drivers studied, skin conductivity and heart rate metrics are closely correlated with driver stress levels. Wan et al. [18] proposed a anger induction method by elicitation events of vehicles weaving/cutting in line, jaywalking, traffic congestion, and waiting at red lights in a real traffic environment. The five physiological features including EEG were extracted for the driving anger identifications. And then a linear discriminant model is employed to detect driving anger by the analysis of receiver operating characteristics. However, the anger arousal degree of the drivers is difficult to control in the real traffic environment, especially with several different elicitation events. Cai et al. [19] investigated emotional behavior of anger, neutral, and excitation of the drivers by collecting driving performance data, psychophysiological responses, and eye movement data in a simulated scenario by using a multiple participant-operated driving simulator. The results demonstrated the feasibility and efficiency of driving simulators to study emotional behavior of the drivers comparing with the actual road rage.

On the other hand, road rage is always associated with gender, age and cognitive ability [9]. Compared to more mature motorists, it was reported that the younger drivers may experience a greater anger, with reacting with more

*The research supported by the National Science Foundation of China (No. 51675224, No. 51775236, and No. U1564214), the National Key Research and Development Program (No. 2017YFB0102600), and the Industrial Innovation Special Fund Project of Jilin Province (No. 2017C045-1).

H. Hu, Z. Zhu, and Z. Gao are with the State Key Laboratory of Automotive Simulation and Control, Changchun, 130000 China (corresponding author to provide phone: +86-0431-8509-5090; e-mail: huhongyu@jlu.edu.cn, 18843102614@163.com, gaozh@jlu.edu.cn).

R. Zheng is with the Institute of Industrial Science, the University of Tokyo, and School of Automotive Engineering, Dalian University of Technology, Dalian 116024, China (e-mail: my_topzrc@yahoo.co.jp).

intense aggression in response to frustrating roadway events [20, 21].

In line with the above background, the motivation of this study is therefore to evaluate different levels of road rage of young drivers, by investigation of physiological characteristics of ECG and EEG signals in a driving simulator experiment.

The remainder of this paper is constructed as follows. Section 2 describes experimental design by application of a driving simulator, including level identification of road rage and physiological signal processing. Consequently, a detailed analysis of physiological characteristics of road rage is presented in section 3, and the conclusion of this study is presented in the final part.

II. METHODOLOGY

A. Participants

All of 12 young adults were recruited for the driving experiment, including 8 males and 4 females. Their ages are between 20 and 24 years old with an average age of 22 years old. All the participants had more than 3-year driving experience. They were in healthy state without heart- and brain-related diseases, and did not take any drugs before the driving test, to avoid influence on the experimental accuracy. All participants were instructed about the testing procedure, and then they signed an informed consent form before a simulator driving experiment.

B. Apparatus

This study was conducted by application of the driving simulator in the State Key Laboratory of Automobile Simulation and Control of Jilin University, taking into account of the potential dangers of on-road experiment and the effective arousal of road anger emotions. It is because that the driving simulator can be used to resemble the driver–vehicle–road environment, and simulate driver behaviors under different traffic conditions without a traffic risk. The driving simulator mainly consists of a cockpit seat, a driving screen with a 120° driving vision, scene generation system, operation system, and data acquisition system. The data were synchronously collected from the accelerator pedal, brake pedal, steering wheel, and steering lamp. A realistic operation system was equipped by a force feedback steering wheel, and a brake with power-assisted feeling, which can provide the subjects with real operation feeling.

In the experiment, the electroencephalogram (EEG) and electrocardiogram (ECG) signals are collected with a sampling rate of 1000 Hz by a wireless physiology recorder system (Biopac MP150, USA). The system consists of biosignal reflector module, conductor module, wireless signal amplifier module, and receiver module. In order to reduce the influence by factors of the external environment, a medical disposable patch electrode is used for the physiology signal collection.

C. Experimental Scenario

A traffic scene of a two-way urban road with four lanes was constructed to test the road rage of driver behaviors by using a PanoSim tool. The PanoSim is a self-developed simulation software platform consisting of vehicle system dynamics, 3D driving environment, traffic environment, vehicle sensors of the camera and radar, wireless communication, GPS, and digital map models. The PanoSim can be applied to develop, test and validate of the related technologies and products for an automotive dynamics performance, automotive electronic control systems, driving assistant system, environmental sensing and autonomous driving in highly fidelity simulation environments.

In the traffic scene, the road is a closed-loop road, including 6 km straight and 1.5 km curve roads, as well as several intersections with traffic lights. The weather was rainy, and traffic density is 20 %. The average speed of traffic flow is 50 km/h. In the experiment, subjects are asked to keep a speed with a range of 50 ± 10 km/h. The driving route is presented in Figure 2.

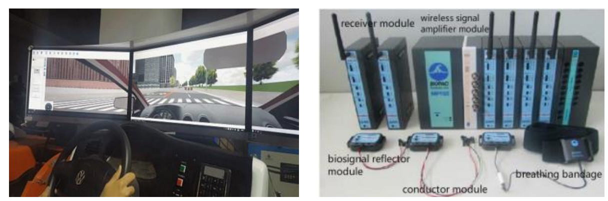

(a) Driving simulator. (b) Wireless physiology recorder.

Figure 1. Experimental platform for the road rage testing: (a) driving simulator, and (b) wireless physiology recorder.

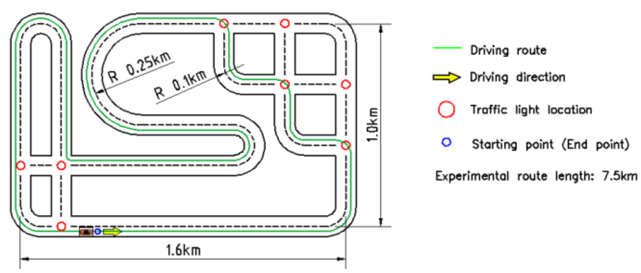

Figure 2. Diagram of the driving route.

D. Experimental Procedure

In the beginning, the experimental requirements and purposes were introduced to subjects, and the subjects registered their basic information and signed the experimental agreement.

In the preparation step, the electrodes were pasted on the head and chest of the subjects, and the signal transmitting module was worn (in figure 3). The EEG and ECG signals were tested by selecting the temporal T3 and T4 electrodes, and the EEG was based on the 10-20 electrode guide alignment standard calibrated by the international electroencephalography association [22]. The arrangement of electrocardiogram (ECG) was sternal lead way to ensure that the signal was clear and stable, while the driver was steering. At the same time, it was processed to perform the adaptive exercise for 10 minutes, for the drivers to adapt to the driving simulator environment.

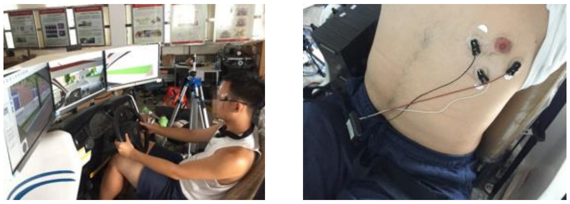

(a) EEG signal collection. (b) ECG signal collection.

Figure 3. A subject's EEG and ECG signals collection in the driving experiment.

In the normal driving, the subjects were driving on a predetermined route without anger triggering, and the normal scenario adopted to record physiological data during the whole process. However, in the angry driving, the normal driving mode was finished, and the anger emotion of the subjects were triggered by watching an unfair incident video.

In anger assessment step, the subjects were asked an inquiry about their anger state with a 2-min interval, after effectively triggering anger. There were four angry levels for subjects to select, and the four levels of evaluation were 1 = normal, 2 = light, 3 = moderate, 4 = heavy. Through the oral inquiries, the subjects' attitude towards the problem was reflected. The anger states inquired every 2 minutes can be collected as the subjective evaluation of anger degree of the subjects.

At the end of the experiment, researchers collated and recorded the data related to the experiment.

E. Data Processing

The EEG and ECG signals of drivers were collected as raw data in the experiment, and therefore it is necessary for effective feature extraction.

At first, noise-signal ratio of original EEG was improved using digital filtering. Then, four typical rhythm bands of α, β, δ, and θ are extracted through a wavelet packet decomposition. At last, frequency domain features of the four typical rhythm bands were obtained with a fast Fourier transform, and then mean power was also calculated for the four typical rhythm bands.

A digital filter of infinite impulse response was used to carry out the band-pass filtering of the EEG signal. The high-pass filter was set at 0.5 Hz, and the low-pass filter was set at 35 Hz. The band processing can effectively filter the interferences of high frequency and low frequency signals.

The recognition rate of the EEG data will be low due to its nonlinear and non-stationary properties, if only a single time- or frequency-domain analysis is used to extract rhythmic features. However, the EEG features can be recognized more effectively by the combination of time-frequency domain than the use of a single analysis. Therefore, wavelet packet decomposition was employed to extract four typical rhythm bands of the EEG data. In addition, wavelet packet decomposition has higher time-frequency resolution than a wavelet decomposition. The EEG data used in this study are normal and angry state signals in a simulator driving environment. The initial sampling frequency of the EEG signal is set to 1000 Hz. The EEG signals in both normal and angry state were pre-processed to remove interference. Then wavelet packet decomposition is used to extract four typical rhythms from the pre-processed EEG signals. The four typical rhythmic waves of EEG ranges in frequency are δ (1–3 Hz), θ (4–7 Hz), α (8–13 Hz), and β (14–30 Hz).

In order to obtain power spectrums of the four typical rhythms, it is also necessary to convert the signals from time-amplitude to frequency - power. The power spectrum is aimed at the power limited signal. It indicates that the signal power changes in the unit band with the frequency. Power spectrums of the four typical rhythm bands are obtained with fast Fourier transform in this paper. The relationship between frequency and power of signals can be obtained through Laplace transform and inverse Laplace transform as,

$$\mathrm{f}(t) = \frac{1}{2\pi}\int_{-\infty}^{\infty} F(\omega)e^{j\omega t} d\omega, \tag{1}$$

$$\mathrm{F}(\omega) = \int_{-\infty}^{\infty} f(t)e^{j\omega t} d\omega. \tag{2}$$

In the case of satisfying the Fourier integral theorem condition, the integral operation of equation (1) is the Fourier transform of $f(t)$. And the integral operation of equation (2) is the inverse Fourier transform of $F(w)$. $F(w)$ is the image function of the Fourier transform. On the contrary, $f(t)$ is the primitive function of $F(w)$.

The rectangular window function is used for the fast Fourier transform, and the length of the time window was set to 2 seconds. The power spectrums of the four rhythmic waves of EEG is obtained. And then the average power in every 2 seconds is calculated, which represents the eigenvalue of the rhythmic wave in 2 seconds. Based on the principle of Fourier analysis, the average power of the signal function $f(t)$ in interval $t \in (-\frac{T}{2}, \frac{T}{2})$ can be expressed as,

$$\mathrm{P} = \lim_{T\to\infty}\int_{-T/2}^{T/2} f^2(t)dt = \frac{1}{2\pi}\int_{-T/2}^{T/2} \lim_{T\to\infty}\frac{|F(\omega)|^2}{T} d\omega \tag{3}$$

where $\frac{|F(\omega)|}{T}$ is a power density function of $f(t)$, and its expression is as,

$$p(\omega) = \lim_{T\to\infty}\frac{|F(\omega)|^2}{T}. \tag{4}$$

It is assumed that the signal $X(\omega)$ is the Fourier transform of the signal $x(t)$, and the discrete Fourier transform of the n point sample data $x(n)$ is $X(K)$

obtained directly from the fast Fourier change. Thereby, the power spectral density of $x(t)$ can be expressed as,

$$p(\omega) = \lim_{T \to \infty} \frac{1}{T} \left| X(\omega) \right|^2 \tag{5}$$

In this paper, the average power diagrams of four typical rhythmic waves of α wave, β wave, δ wave and θ wave are obtained by using a fast Fourier transform. As shown in Figure 4, the power diagram is demonstrated with the four rhythmic waves of the measured EEG data.

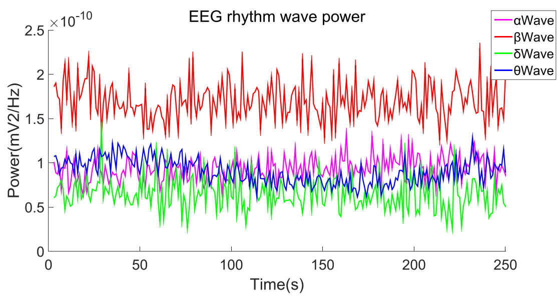

Figure 4. Examples of the EEG rhythm wave power.

For the ECG signal, the impurity wave was filtered by a digital filter, and then the average heart rate (AHR) and R-R standard deviation (SD) were obtained by a time domain analysis. According to the position of R wave detected in the temporal, the R wave can be then converted to the AHR. The number of R-R in the time interval t can be expressed as N_t and the average heart rate of this time interval t can be denoted as

$$AHR = \frac{60 \times N_t}{t} . \tag{6}$$

For R-R standard deviation, the R-R standard deviation is calculated after the position of R wave is obtained by time domain analysis as,

$$SD = \sqrt{\frac{1}{n} \sum_{i=1}^{n} (R_i - \overline{R})^2} . \tag{7}$$

where $\overline{R}$ is the average of R-R, R_i is the i th R-R, n is the n selected R-R, and SD is the standard deviation of the R-R. The examples of the AHR and R-R interval are presented in figures 5 and 6, respectively.

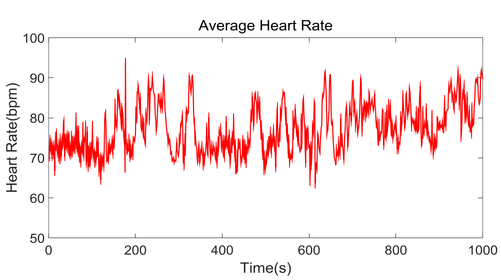

Figure 5. Example of the average heart rate.

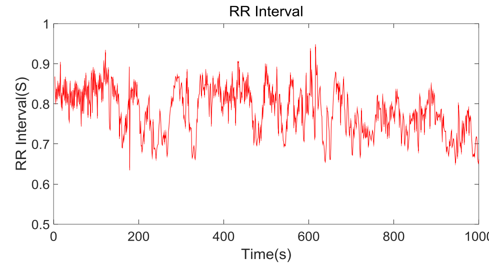

Figure 6. Example of the R-R interval.

Due to differences of skin resistance between individuals, it is crucial to normalize or standardize the measure biosignals. In this paper, we normalized the EEG and ECG data with formula (8). In this way, several standardize features of α, β, δ, θ *and AHR* can be calculated to compare and analyze for different individuals. R-R standard deviation is already a standard feature which need not to do this step to normalize.

$$data\_sta_i = \frac{data_i - data_{\min}}{data_{\min}} \tag{8}$$

where $data_i$ is the i th sample data of a biosignal, $data_{\min}$ is minimum sample data of the biosignal, and $data\_sta_i$ represents the standardize data of the biosignal.

III. Results and Discussions

A. Average Power of the Brain Wave

In figure 7, the results of the standardize feature of α wave are presented for four different angry degrees, and a one-way repeated measure ANOVA was processed for statistical analyses of the four variables of normal, light, moderate, and heavy anger degrees. At the 0.05 confidence level, there was a significant difference between the four samples (F = 2.19, p = 8.76E-02 < 0.05), indicating that the standardize feature of α wave was significant different for the normal state (M = 1.37, SD = 0.41), light anger (M = 1.50, SD = 0.54), moderate anger (M = 1.44, SD = 0.54), and heavy anger (M = 1.41, SD = 0.58).

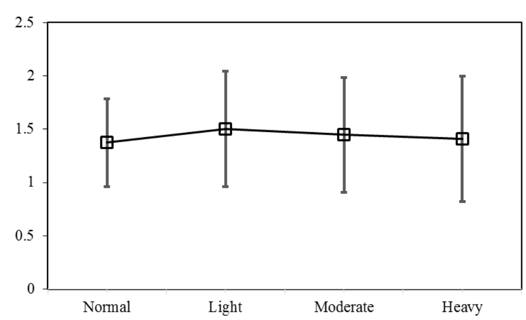

Figure 7. Standardize features of α wave.

In figure 8, the results of the standardize feature of β wave are presented for four different angry degrees, and a one-way repeated measures ANOVA was processed for statistical analyses of the four variables of normal, light, moderate, and heavy anger degrees. At the 0.05 confidence level, there was a significant difference between the four samples ($F = 7.95$, $p = 3.16E-05 < 0.05$), for the normal state ($M = 1.30$, $SD = 0.42$), light anger ($M = 1.29$, $SD = 0.37$), moderate anger ($M = 1.37$, $SD = 0.48$), and heavy anger ($M = 1.48$, $SD = 0.48$).

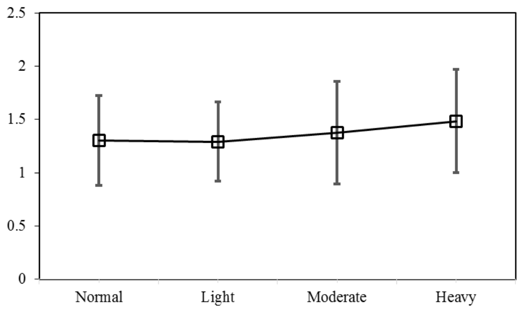

Figure 8. Standardize features of β wave.

In figure 9, the results of the standardize feature of δ wave are presented for four different angry degrees, and a one-way repeated measures ANOVA was processed for statistical analyses of the four variables of normal, light, moderate, and heavy anger degrees. At the 0.05 confidence level, there was a significant difference between the four samples ($F = 8.47$, $p = 1.52E-05 < 0.05$), indicating that the standardize feature of δ wave was significant different for the normal state ($M = 5.10$, $SD = 1.74$), light anger ($M = 6.27$, $SD = 2.75$), moderate anger ($M = 5.88$, $SD = 3.42$), and heavy anger ($M = 5.25$, $SD = 2.47$).

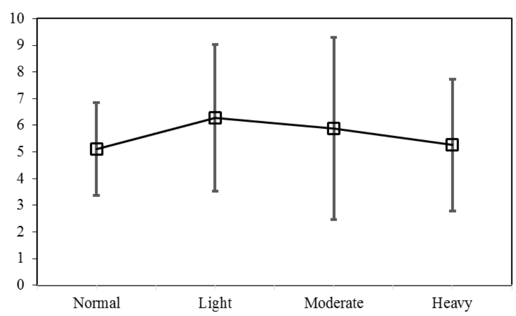

Figure 9. Standardize features of δ wave.

In Figure 10, the results of the standardize feature of θ wave are presented for four different angry degrees, and a one-way repeated measures ANOVA was processed for statistical analyses of the four variables of normal, light, moderate, and heavy anger degrees. At the 0.05 confidence level, there was no significant difference between the four samples ($F = 0.58$, $p = 6.30E-01 > 0.05$), indicating that the standardize feature of θ wave was no significant different for the normal state ($M = 2.89$, $SD = 3.01$), light anger ($M = 3.06$, $SD = 1.17$), moderate anger ($M = 3.09$, $SD = 2.93$), and heavy anger ($M = 2.85$, $SD = 1.00$).

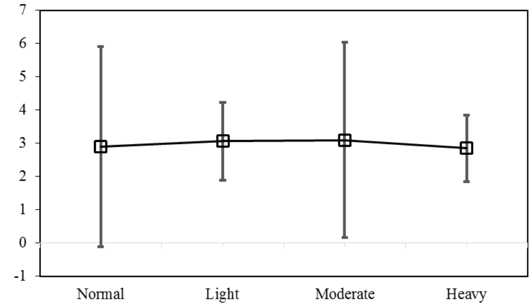

Figure 10. Standardize features of θ wave.

B. Analyses of Electrocardiograph Signal

In figure 11, the results of standardize features of the AHR are presented for four different angry degrees, and a one-way repeated measures ANOVA was processed for statistical analyses of the four variables of normal, light, moderate, and heavy anger degrees. At the 0.05 confidence level, there was a significant difference between the four samples ($F = 44.89$, $p = 8.32E-27 < 0.05$), indicating that the AHR was significant different for the AHR of the normal state ($M = 0.42$, $SD = 0.13$), light anger ($M = 0.42$, $SD = 0.17$), moderate anger ($M = 0.46$, $SD = 0.17$), and heavy anger ($M = 0.58$, $SD = 0.15$).

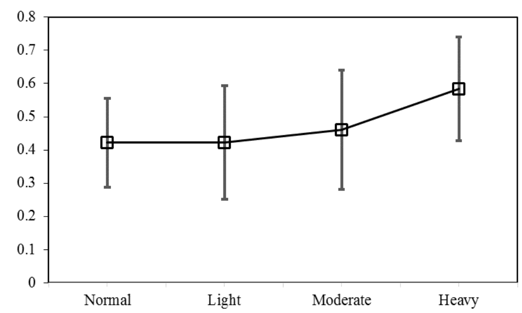

Figure 11. Standardize features of average heart rate.

As shown in figure 12, the results of the R-R standard deviation are collected for the different angry degrees. At the 0.05 confidence level, a one-way repeated measures ANOVA was processed for statistical analyses of the four variables of normal, light, moderate, and heavy anger degrees. For the R-R standard deviation, there is a main effect of the angry state ($F = 10.21$, $p < 0.001$), indicating that the R-R standard deviation was significantly different for the normal state ($M = 0.030738464$, $SD = 0.008903055$), light anger ($M = 0.03614828$, $SD = 0.008693138$), moderate anger ($M = 0.044543539$, $SD = 0.009289295$), and heavy anger ($M = 0.052308061$, $SD = 0.010490805$).

The post hoc tests showed that the R-R standard deviation of heavy anger was significantly higher than that of light anger ($p = 0.002 < 0.01$) and normal state ($p < 0.001$). Moreover, the R-R standard deviation of moderate anger was significantly higher than that of normal state ($p = 0.012 < 0.05$).

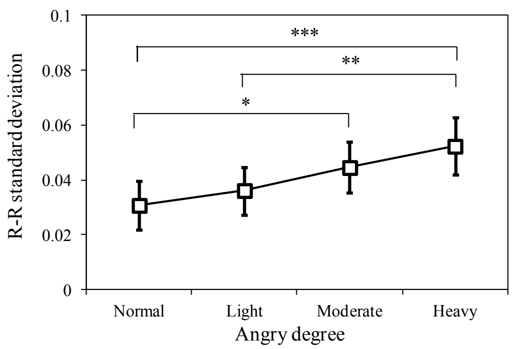

Figure 12. R-R standard deviation (*p < 0.05, **p < 0.01, and *** p < 0.001).

IV. CONCLUSION

This paper studies the relationship between the anger emotions and the physiological information of young drivers based on a driving simulator experiment. Through reasonable design of anger trigger experiment, this paper extracted physiology features of EEG, R-R standard deviation, and AHR in the driving anger state. Through analysis the standardize features calculated from the raw data, it is concluded that by ANOVA test, the five indicators, including α, β, δ , AHR and R-R standard deviation, have significant differences in the four samples obtained from four different anger states.

The research results are valuable to study the drivers' emotional state recognition of and intelligent human-machine interaction in the future. On the basis of this article, the future research work mainly focuses on the following aspects:

(1) The difference of physiological information among different individuals is obvious. However, the driving experiment was only conducted with 12 young drivers. Therefore, future research will further increase the test sample and make a comparative analysis of different types of people, considering sex, age, and driving experience.

(2) Human emotion is a complex psychological state of many kinds and dimensions. People in the face of different changes in stress will trigger a variety of different emotions. Further insight on physiological expression of multidimensional emotion is necessary.

References

[1] C. Pêcher, C. Lemercier, M. J. Cellier, X. Cuny, and C. Chauvin, "Emotions drive attention: effects on driver's behaviour," *Safety Science*, vol. 47, no. 9, pp. 1254-1259, 2009.

[2] P. Wan, C. Wu, Y. Lin, and X. Ma, "Optimal threshold determination for discriminating driving anger intensity based on EEG wavelet features and ROC curve analysis," *Information*, vol. 7, no. 3, pp. 1-17, 2016.

[3] W. Vanlaar, H. Simpson, D. Mayhew, and R. Robertson, "Aggressive driving: a survey of attitudes, opinions and behaviors," *Journal of Safety Research*, vol. 39, no. 4, pp. 375-381, 2008.

[4] M. Danaf, M. Abou-Zeid, and I. Kaysi, "Modeling anger and aggressive driving behavior in a dynamic choice-latent variable model," *Accident Analysis & Prevention*, 75:105-118, 2015.

[5] L. J. Deffenbacher, M. D. Deffenbacher, S. R. Lynch, and L.T. Richards, "Anger, aggression, and risky behavior: a comparison of high and low anger drivers," *Behaviour Research & Therapy*, vol. 41, no. 6, pp. 701-718, 2003.

[6] C. Chai and X. Wu, "Gender differences in driving anger emotional susceptibility," in *IEEE International Symposium on Computational Intelligence and Design*, 2016, pp. 590-593.

[7] R. E. Dahlen, C. R. Martin, K. Ragan, and M. M. Kuhlman, "Driving anger, sensation seeking, impulsiveness, and boredom proneness in the prediction of unsafe driving," *Accid. Anal. Prev.*, vol. 37, no. 2, pp. 341-348, 2005.

[8] N. A. Stephens and A. J. Groeger, "Following slower drivers: lead driver status moderates driver's anger and behavioural responses and exonerates culpability," *Transp. Res. Part F*: *Traffic Psychology & Behaviour*, vol. 22, pp. 140–149, 2014.

[9] M. C. Wickens, E. R. Mann R E, G. Stoduto, A. Lalomiteanu, and R. G. Smart, "Age group differences in self-reported aggressive driving perpetration and victimization," *Transportation Research Part F*: *Traffic Psychology & Behaviour*, vol. 14, no. 5, pp. 400-412, 2011.

[10] C. Dobbins and S. Fairclough, "A mobile lifelogging platform to measure anxiety and anger during real-life driving," in *IEEE International Conference on Pervasive Computing and Communications Workshops*, 2017, pp. 327-332.

[11] NHTSA, "Traffic safety facts 2010: A compilation of motor vehicle crash data from the fatality analysis reporting system and the general estimates system," *Washington DC*: *National Highway Traffic Safety Administration*, 2010.

[12] P. J. Depasquale, S. E. Geller, W. S. Clarke, L. C. Littleton, "Measuring road rage: development of the propensity for angry driving scale," *Journal of Safety Research*, vol. 32, no. 1, pp. 1-16, 2001.

[13] J. Mesken, M. P. Hagenzieker, T. Rothengatter, and D. de Waard, "Frequency, determinants, and consequences of different drivers' emotions: An on-the-road study using self-reports, (observed) behaviour, and physiology," *Transportation Research Part F*: *Traffic Psychology* & *Behaviour*, vol. 10, no. 6, pp. 458-475, 2007.

[14] R. Abdu, D. Shinar, and N. Meiran, "Situational (state) anger and driving," *Transportation Research Part F*: *Psychology* & *Behaviour*, vol. 15, no. 5, pp. 575-580, 2012.

[15] D. C. Katsis, Y. Goletsis, G. Rigas, and D.I. Fotiadis, "A wearable system for the affective monitoring of car racing drivers during simulated conditions," *Transportation Research Part C*: *Emerging Technologies*, vol. 19, no. 3, pp. 541-551, 2011.

[16] M. Zhao, F. Adib, and D. Katabi, "Emotion recognition using wireless signals," in *International Conference on Mobile Computing and Networking*, 2016, pp. 95-108.

[17] A. J. Healey and W. R. Picard, "Detecting stress during real-world driving tasks using physiological sensors," *IEEE Transactions on Intelligent Transportation Systems*, vol. 6, no. 2, pp. 156-166, 2005.

[18] P. Wan, C. Wu, Y. Lin, and X. Ma, "On-road experimental study on driving anger identification model based on physiological features by ROC curve analysis," *IET Intelligent Transport Systems*, vol. 11, no. 5, pp. 290-298, 2017.

[19] H. Cai, Y. Lin, and R. Mourant, "Study on driver emotion in driver-vehicle-environment systems using multiple networked driving simulators," in *Driving Simulation Conference*, 2007.

[20] T. Lajunen and D. Parker, "Are aggressive people aggressive drivers? A study of the relationship between self-reported general aggressiveness, driver anger and aggressive driving,"*Accident Analysis and Prevention*, vol. 33, no. 2, pp. 243-55, 2001.

[21] R. Smart, G. Stoduto, R. Mann, and E. Adlaf, "Road rage experience and behavior: vehicle, exposure, and driver factors," *Journal of Crash Prevention & Injury Control*, vol. 5, no. 4, pp. 343-348, 2004.

[22] W. R. Homan, J. Herman, and P. Purdy, "Cerebral location of international 10–20 system electrode placement," *Electroencephalography and Clinical Neurophysiology*, vol. 66, no. 4, pp. 376-382, 1987.